Dissipative light bullets in an optical parametric oscillator

Nikolay Veretenov[1] and Mustapha Tlidi[2]
[1]*S. I. Vavilov State Optical Institute, Institute for Laser Physics, St. Petersburg, 199034 Russia*
[2]*Optique Nonlinéaire Théorique, Université Libre de Bruxelles, Campus Plaine, CP 231, B-1050 Bruxelles, Belgium*
(Received 5 April 2009; published 25 August 2009)

When chromatic dispersion operates together with two-dimensional diffraction, the degenerate optical parametric oscillator exhibits three-dimensional (3D) localized structures in a regime devoid of Turing or modulational instabilities. They consist of single lamella, cylinder, or light drops. These 3D structures are generated spontaneously from a weak random noise. We construct 3D bifurcation diagrams associated with these structures. We show that a single cylinder and a single light drop exhibit an overlapping domain of stability. Finally, for a large input intensity, we identify a self-pulsing behavior affecting the stability of 3D localized structures.

DOI: 10.1103/PhysRevA.80.023822 PACS number(s): 42.65.Tg, 42.65.Sf, 42.60.Da

I. INTRODUCTION

Self-organization process leading to a spontaneous formation of dissipative structures is a universal phenomenon observed in a wide variety of natural nonlinear systems such as biology, chemistry, fluid mechanics, ecology, and nonlinear optics [1–5]. Recently, significant advances have been made in the study of transverse optical localized structures often called cavity solitons [6,7]. These are largely due to research in nonlinear optical settings, where cavity solitons have potential applications as bits for information storage and processing. Experimental evidence of two-dimensional (2D) localized structures in nonlinear planar cavities has reinforced the interest in this area of research [8–16].

On one hand, the coupling between nonlinearity and diffraction leads to the formation of dissipative localized structures that can be classified as follows: depending on the critical value of the most instable wave number k_T at the Turing or the modulational instability, (i) if $k_T=O(1)$, and if the Turing bifurcation appears subcritical, then stable localized structures can be generated in the pinning range involving self-organized periodic structures and a single homogeneous steady state. The commutation process associated with optical bistability is not a necessary condition for the generation of stable localized structures [17,18]. The link between subcritical Turing instability and the formation of localized structures were established first in passive nonlinear resonators [18–20,26] and in quadratic media [21–25]. (ii) If $k_T \rightarrow 0$, the modulational instability occurs close to the limit point associated with a domain of bistability. The long-wavelength pattern forming process is altered and leads to the spontaneous formation of localized structures [27]. (iii) If $k_T=0$, i.e., the homogeneous steady states are stable with respect to the Turing bifurcation. In this case, localized structures can be generated spontaneously from a weak noise. The stabilization of these structures often called phase solitons is attributed to phase indetermination in bistable systems. Bistable behavior between two stable homogeneous steady states becomes a necessary condition for the existence of phase solitons [28–36].

On the other hand, in the purely temporal regime, the chromatic dispersion plays a central role in the formation of time dissipative structures and fronts [37–39]. These structures have important possible applications for the development of high bit-rate optical communication and passively mode locked lasers. In this case, the intracavity field is spatially homogeneous by using a guided wave structures, and therefore diffraction does not play any role.

When diffraction and chromatic dispersion have a comparable influence in the nonlinear resonators, three-dimensional (3D) localized structures are formed. They consist of either self-organized lattices or localized light drops traveling at the group velocity of the light within the cavity. They are often called light bullets in the case of conservative systems [40,41] where the stabilization is achieved by a balance among focusing nonlinearity, 2D diffraction, and dispersion. By using a multiscale analysis, Leblond derived a 3D model to describe the propagation of short pulses in quadratic media [42]. He also discussed the validity of that model by taking into account the walkoff, the phase mismatch, and the anisotropy [42]. In dissipative systems, such as nonlinear resonators, we shall adopt the terminology "dissipative light bullets" proposed recently by Akhmediev *et al.* [43]. In order to avoid the problem of beam collapse, a saturable nonlinearity [44] or an optical cavity [45] is used. Laser bullets belong to the class of 3D dissipative localized structures, which have been found in active systems [40]. Dissipative light bullets have been studied in the nonlinear Kerr cavity [45–47], in the optical parametric oscillator [48], in the type II second-harmonic generation [49–51], in the wide-aperture laser with saturable absorber [52–54], and in the complex cubic-quintic Ginzburg-Landau equation [55,56]. Recently, dissipative light bullets have been found in a non-mean-field model describing a nonlinear resonator with a saturable absorber [57,58]. Excellent overview of dissipative light bullets are given by Rosanov [2].

In this paper, we consider a diffractive and dispersive degenerate optical parametric oscillator (DOPO). All previous works reported on dissipative light bullets in that system have been performed in regimes where one or more steady states exhibit a pattern forming instability. In the present work, we focus on dissipative light bullets in a regime devoid of pattern forming instability. We show the existence of stable 3D localized structures consisting of a single lamella, a cylinder, or light drops (or bullets). Some of these structures have been previously reported in the special case of nascent bistability where the dynamics is described by the

Swift-Hohenberg equation [48]. Here, we study the full DOPO mean-field model. The 3D dissipative light bullets are robust since they are generated spontaneously from a weak initial noise. We construct a 3D bifurcation diagrams for a single lamella, a cylinder, and a light drop. We show that there is an overlapping domain of stability between a single cylinder and a light drop. Finally, when we increase further the intensity of the input field, 3D dissipative light bullets exhibit a time self-pulsation behavior.

The paper is organized as follows. After briefly introducing the DOPO mean-field model and presenting the linear stability analysis (Sec. II), we present the full numerical simulations of the model equations showing stable dissipative light bullets and 3D bifurcation diagrams associated with a single lamella, a cylinder, and a light drop (Sec. III). We conclude in Sec. IV.

II. MEAN-FIELD MODEL

Frequency conversion by means of optical parametric conversion is a fundamental phenomenon for the generation of tunable coherent radiation in $\chi^{(2)}$ medium. The optical parametric oscillator is a promising device in several applications, ranging from the generation of nonclassical states of light to detection, to optical coherent information processing, and to spectroscopy [59,60]. We consider the type I parametric amplification that does not involve polarization degrees of freedom generated by the birefringence of the quadratic crystal. The propagation equations for the pump and the signal amplitudes are

$$\frac{\partial u_1}{\partial z} + \frac{n_1}{c}\frac{\partial u_1}{\partial t} = \frac{i\omega\chi^{(2)}}{c\eta_1}u_2 u_1^* + i\frac{c}{2\omega n_1}\Delta_\perp u_1 + i\beta_1\frac{\partial^2 u_1}{\partial \tau^2}, \quad (1)$$

$$\frac{\partial u_2}{\partial z} + \frac{n_2}{c}\frac{\partial u_2}{\partial t} = \frac{i\omega\chi^{(2)}}{2c\eta_2}u_1^2 + i\frac{c}{\omega n_2}\Delta_\perp u_2 + i\beta_2\frac{\partial^2 u_2}{\partial \tau^2}, \quad (2)$$

where u_1 and u_2 are the normalized slowly varying complex envelopes of the signal and the pump fields at frequencies ω and $\omega/2$, respectively. The time t, describes the slow evolution of the field envelopes; τ is the normalized time in reference frame traveling at the group velocity of the light. The parameters $n_{1,2}$ and $\eta_{1,2}$ are the index of refraction and the characteristic impedance associated with the pump and the signal fields, respectively. Diffraction is described by the Laplace operator $\Delta_\perp = \partial^2/\partial x^2 + \partial^2/\partial y^2$ acting on the transverse plane (x,y) orthogonal to the longitudinal direction z, and chromatic dispersion is modeled by the second derivative with respect to the fast time τ. The dispersion coefficients of the signal and the pump fields are β_1 and β_2, respectively, and c is the speed of light.

The device we consider consists of a ring cavity filled with $\chi^{(2)}$ medium and driven by an external coherent beam S at the frequency ω as shown in Fig. 1. The propagation equations (1) and (2) with appropriate boundary conditions at the mirrors can be reduced to the following partial differential equations [61]:

$$\frac{\partial u_1}{\partial t} = -(1+i\delta_1)u_1 + u_2 u_1^* + i\left(a_1\Delta_\perp + \beta_1\frac{\partial^2}{\partial \tau^2}\right)u_1, \quad (3)$$

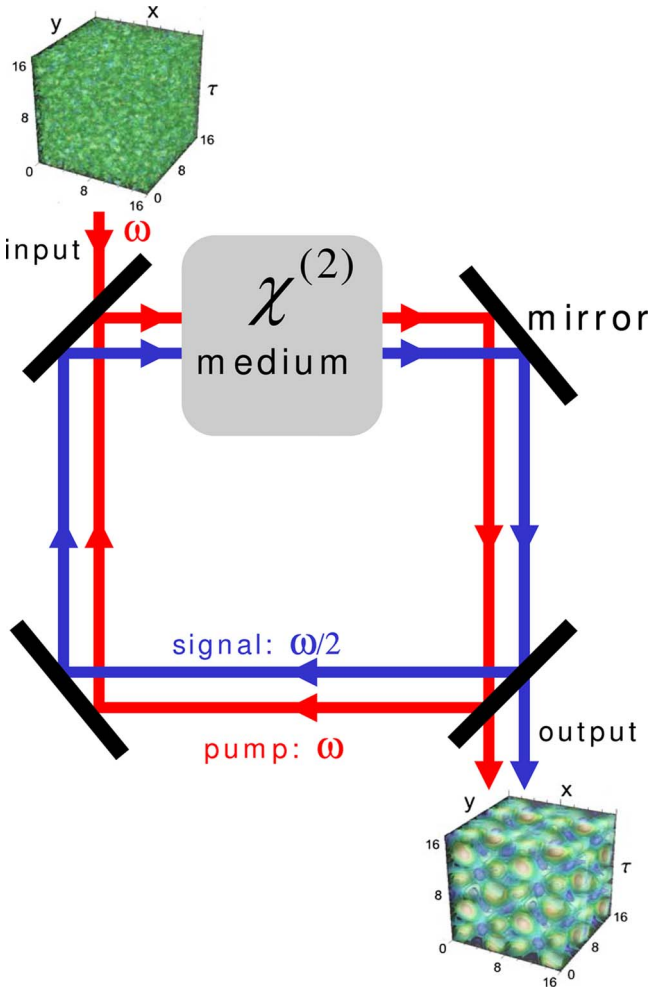

FIG. 1. (Color online) Schematic setup of a ring cavity resonator filled with quadratic medium and driven by a coherent radiation beam S at frequency ω. Pump and signal fields are coupled by the $\chi^{(2)}$ crystal.

$$\frac{\partial u_2}{\partial t} = -(1+i\delta_2)u_2 - u_1^2 + S + i\left(a_2\Delta_\perp + \beta_2\frac{\partial^2}{\partial \tau^2}\right)u_2. \quad (4)$$

The parameters $\delta_{1,2}$ are the detuning at both frequencies. The diffraction coefficients of the signal and the pump fields are a_1 and a_2, respectively. Equations (3) and (4) have been derived in the framework of mean-field approximation which means that (i) the length of the cavity is much shorter than the characteristic diffraction and dispersion lengths of the pump and the signal fields; (ii) high finesse resonator and (iii) both cavity detuning and nonlinear cavity phase shift should be smaller than unity. This last condition comes from the fact that external power can be coupled into the cavity only if the system is close to resonance.

Equations (3) and (4) have two types of homogeneous steady-state solutions: (a) nonlasing state $u_1=0$ and $u_2 = S/(1+i\delta_2)$ and (b) lasing state $S^2=(1+\delta_1^2)(1+\delta_2^2) + 2(1-\delta_1\delta_2)|u_1|^2+|u_1|^4$ and $|u_2|^2=1+\delta_1^2$. The two homogeneous solutions coincide at the lasing threshold $S^2=S_{th}^2 = (1+\delta_1^2)(1+\delta_2^2)$. The nonlasing solution undergoes the pitchfork bifurcation at the point $S=S_{th}$. The linear stability analy-

sis of the homogeneous states (a) and (b) with respect to perturbations of the form $\exp(i\mathbf{k}\cdot\mathbf{r}-\lambda t)$ with $\mathbf{k}=(k_x,k_y,k_\tau)$ and $\mathbf{r}=(x,y,\tau)$, which are compatible with wide-aperture cavity, i.e., a large Fresnel number systems, shows that the Turing instability occurs when one of the eigenvalues of the linear operator vanishes. This happens when

$$4|u_1|^4 + 4|u_1|^2[\alpha_1(1-\alpha_2)+\alpha_2] + \alpha_2(\alpha_1 - |u_2|^2) = 0, \quad (5)$$

$$\alpha_{1,2} = 1 + [\delta_{1,2} + a_{1,2}(k_x^2 + k_y^2) + \beta_{1,2}k_\tau^2]^2. \quad (6)$$

From this equation, we see that the nonlasing solution (a) becomes instable with respect to a Turing instability in the range $S_T<S<S_{th}$, with $S_T=\sqrt{1+\delta_2^2}$. At the Turing instability point ($S=S_T$), the most unstable wave number is given by $a_1(k_x^2+k_y^2)+\beta_1 k_\tau^2=-\delta_1$. These modes form an ellipsoid in the Fourier space (k_x,k_y,k_τ), when a_1 and β_1 have the same sign, and a hyperboloid for opposite signs. Here, we consider only the anomalous dispersion regime, i.e., $\beta_{1,2}>0$. In order to study the stability of the lasing state (b), let us assume that, $\delta_2=\delta_1/2$ and $\beta_2=\beta_1/2$. In addition, the phase-matching condition imposes that $a_2/a_1=1/2$. Under these assumptions, the critical wavelength is $a_1(k_x^2+k_y^2)+\beta_1 k_\tau^2=-\delta_1+\sqrt{(4-\delta_1^2)/[2(4|u_{1T}|^2-1)}$ and the threshold associated by the Turing instability; $|u_{1T}|^2$ satisfies the following cubic equation: $(4+\delta_1^2)^2+64|u_{1T}|^2(4|u_{1T}|^4+3|u_{1T}|^2-1-\delta_1^2)=0$. In what follows we focus on a situation usually realized experimentally, namely, a near resonance condition, i.e., $\delta_{1,2}=0$. In that case the above linear stability analysis of the homogeneous solutions shows that both lasing (b) and nonlasing (a) states are stable with respect to Turing instability.

III. THREE-DIMENSIONAL STRUCTURES AND BIFURCATION DIAGRAMS

We have performed numerical simulations of the full DOPO model equations (3) and (4) taking into account 2D diffraction and chromatic dispersion. The numerical simulations are based on a finite-difference method. More precisely, the Crank-Nikolson scheme is used with periodic or Neumann boundary condition in (x,y,τ) directions. The initial condition consists of a small noise with an amplitude of 10^{-5} added to the unstable homogeneous nonlasing state (a). Integration mesh varies from $30\times30\times30$ to $80\times80\times80$ with a step size of 0.1–0.3. In the earlier time evolution, the signal field amplitude displays a random distribution of small size domains. During the time evolution, these domains slowly grow and deform. Some of these 3D domains disappear. As the time further increases, the dynamics leads to the formation of crossing cylinders as shown in Fig. 2 at $t=25$. For a late time evolution, the dynamics leads spontaneously to a stationary state which consists of stable light drops or bullets. The spontaneous time evolution toward the formation of this 3D structures is shown in Fig. 2. To visualize 3D light bullets, we draw isosurfaces, corresponding to zero real part of the signal field u_1. In order to study numerically the stability of 3D localized structures (LSs), we first consider the simplest solution, namely, a single lamella. The bifurcation diagram associated with this solution is shown in Fig. 3. We

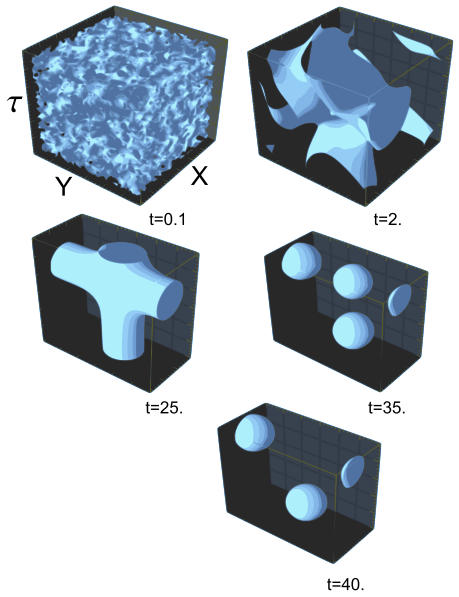

FIG. 2. (Color online) Isosurfaces associated with the signal field amplitude $|u_1|$ showing the time evolution of robust stable light drops in the (x,y,τ) space obtained numerically from a random initial condition. Parameters are $\delta_{1,2}=0$, $\beta_2=\beta_1/2=1$, $a_2=a_1/2=1$, and $S=4$.

used the same integration method and the same initial condition as for light drops (cf. Fig. 2). The amplitude of the lamella increases as the input field amplitude increases as shown in the bifurcation (Fig. 3). The single lamella structure becomes unstable when the input field $S>S_{cr}$ and the branch of a single lamella undergoes a time oscillation (Hopf bifurcation). The maximum and the minimum of these peri-

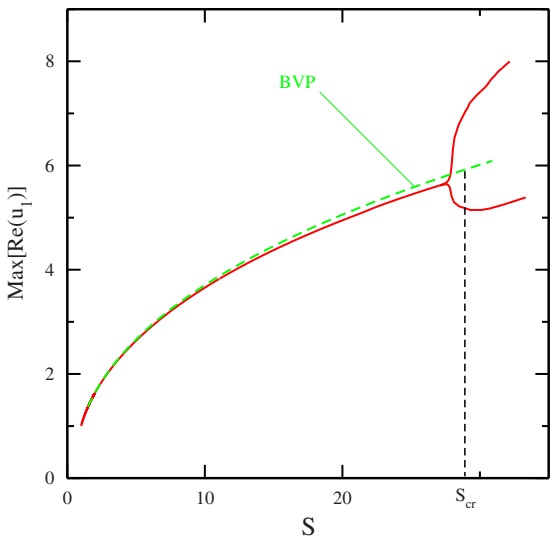

FIG. 3. (Color online) Bifurcation diagram associated with a single lamella. Parameters are $\delta_{1,2}=0$, $\beta_2=\beta_1/2=1$, $a_2=a_1/2=1$, and $S=3$. The broken line indicates the semianalytical solutions obtained by solving the boundary value problem (BVP) associated with model (3) and (4) with the Neumann boundary conditions. The full line curve indicates the solutions obtained by numerical simulations of Eqs. (3) and (4).

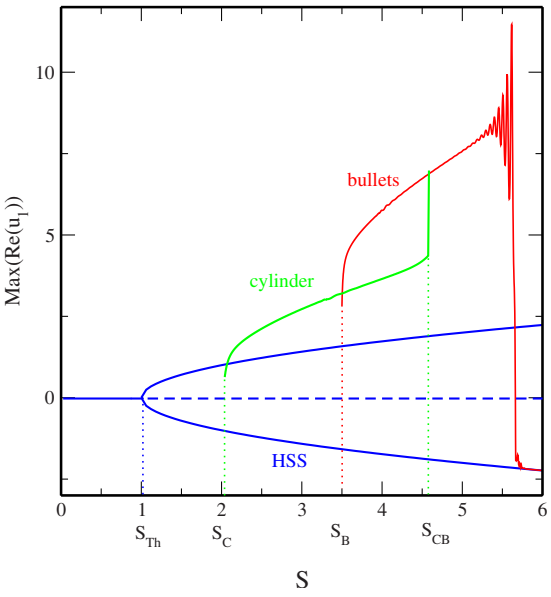

FIG. 4. (Color online) Bifurcation diagram associated with single cylinder and light bullet. Parameters are the same as in Fig. 2.

odic oscillations in time are plotted in red of Fig. 3. We check this full 3D numerical simulation by solving the boundary value problem associated with Eqs. (3) and (4) with the Neumann boundary conditions. This is because a single lamella is essentially a one-dimensional structure. The results of these calculations are plotted in green dotted line of Fig. 3. Stability analysis of the lamella is performed by linearizing Eqs. (3) and (4) around the single lamella solution and by solving the eigenvalue problem. This method allows us to estimate the threshold associated with the self-pulsing instability (Hopf bifurcation) $S=S_{cr}\approx 29$. This semi-analytical estimation is rather good when comparing with 3D numerical simulations of the full DOPO mean-field model. The 3D bifurcation diagram associated with a single cylinder and light bullets is shown in Fig. 4. By varying the input field intensity, the single cylinder appears spontaneously in the range $S_C<S<S_B$. At $S=S_B$, a transition from a single cylinder branch of solution toward the light bullet solutions occurs at $S=S_{CB}$ as shown in Fig. 4. When increasing the input field intensity from $S=S_{CB}$, the light bullet survives and we see clearly an overlapping domain of stability between a

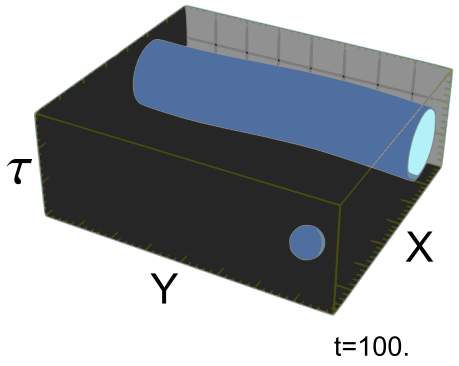

FIG. 5. (Color online) Isosurfaces associated with the signal field amplitude $|u_1|$ showing a coexistence between single cylinder and light bullet. Parameters are $\delta_{1,2}=0$, $\beta_2=\beta_1/2=1$, $a_2=a_1/2=1$, and $S=3$. Periodic boundary conditions are used in both directions.

single cylinder and a light bullet in the parameter range $S_B<S<S_{CB}$. For large intensity, the light bullet solutions undergo, as for the single lamella, time oscillations associated with the Hopf bifurcation. In the range $S_B<S<S_{CB}$, by using an appropriate initial condition, we can generate a coexistence of a single cylinder and a single light bullet. This feature is illustrated in Fig. 5.

IV. CONCLUSIONS

We have demonstrated numerically the formation of stable dissipative light bullets in the dispersive and diffractive degenerate optical parametric oscillator. We have constructed bifurcation diagrams associated with a single lamella, a single cylinder, and a light bullet. These diagrams give an information on the stability domain of these structures, and they also show a coexistence between a single cylinder and a light bullet. Finally, we show a dynamical regime associated with a time-oscillatory instability affecting the stability of dissipative light bullets.

ACKNOWLEDGMENTS

We would like to thank very much N. N. Rosanov and A. G. Vladimirov for their comments and remarks that significantly improved the manuscript. We thank also T. Kolokolnikov for fruitful discussions. M.T. is supported by Fonds de la Recherche Scientifique (F.R.S.)-FNRS, Belgium.

[1] P. Glansdorff and I. Prigogine, *Thermodynamic Theory of Structures, Stability and Fluctuations* (Wiley, New York, 1971); E. Meron, Phys. Rep. **218**, 1 (1992); J. Chanu and R. Lefever, Physica A **213**, xiii (1995); M. C. Cross and P. C. Hohenberg, Rev. Mod. Phys. **65**, 851 (1993); R. Kapral and K. Showalter, *Chemical Waves and Patterns* (Kluwer Academic Press, Dordrecht, 1995).

[2] N. N. Rosanov, Prog. Opt. **35**, 1 (1996); N. N. Rosanov, *Spatial Hysteresis and Optical Patterns* (Springer, Berlin, 2002).

[3] K. Staliunas and V. J. Sanchez-Morcillo, *Transverse Patterns in Nonlinear Optical Resonators*, Springer Tracts in Modern Physics (Springer-Verlag, Berlin, 2003); L. A. Lugiato, IEEE J. Quantum Electron. **39**, 193 (2003); Y. S. Kivshar and G. P. Agrawal, *Optical Solitons: From Fiber to Photonic Crystals* (Academic Press, Elsevier Science, Amsterdam, 2003); N. Akhmediev and A. Ankiewicz, *Dissipative Solitons*, Lecture Notes in Physics Vol. 661 (2005).

[4] M. Tlidi, T. Kolokolnikov, and M. Taki, Chaos **17**, 037101

(2007).
[5] N. Akhmediev and A. Ankiewicz, *Dissipative Solitons: From Optics to Biology and Medicine* (Springer-Verlag, Berlin, 2008).
[6] M. Saffman, D. Montgomery, and D. Z. Anderson, Opt. Lett. **19**, 518 (1994).
[7] V. B. Taranenko, K. Staliunas, and C. O. Weiss, Phys. Rev. A **56**, 1582 (1997).
[8] V. B. Taranenko, K. Staliunas, and C. O. Weiss, Phys. Rev. Lett. **81**, 2236 (1998); V. B. Taranenko, I. Ganne, R. J. Kuszelewicz, and C. O. Weiss, Phys. Rev. A **61**, 063818 (2000).
[9] S. Barland, J. R. Tredicci, M. Brambilla, L. A. Lugiato, S. Balle, M. Guidici, T. Maggipinto, L. Spinelli, G. Tissoni, T. Knodl, M. Miller, and R. Jager, Nature (London) **419**, 699 (2002).
[10] M. Pesch, E. Grosse Westhoff, T. Ackemann, and W. Lange, Phys. Rev. Lett. **95**, 143906 (2005).
[11] X. Hachair, L. Furfaro, J. Javaloyes, M. Giudici, S. Balle, J. Tredicce, G. Tissoni, L. A. Lugiato, M. Brambilla, and T. Maggipinto, Phys. Rev. A **72**, 013815 (2005).
[12] M. G. Clerc, A. Petrossian, and S. Residori, Phys. Rev. E **71**, 015205(R) (2005); U. Bortolozzo, L. Pastur, P. L. Ramazza, M. Tlidi, and G. Kozyreff, Phys. Rev. Lett. **93**, 253901 (2004).
[13] E. Louvergneaux, F. Rogister, and P. Glorieux, Phys. Rev. Lett. **99**, 263901 (2007).
[14] D. Bajoni, E. Semenova, A. Lemaître, S. Bouchoule, E. Wertz, P. Senellart, S. Barbay, R. Kuszelewicz, and J. Bloch, Phys. Rev. Lett. **101**, 266402 (2008).
[15] X. Hachair, G. Tissoni, H. Thienpont, and K. Panajotov, Phys. Rev. A **79**, 011801(R) (2009).
[16] P. Genevet, S. Barland, M. Giudici, and J. R. Tredicce, Phys. Rev. Lett. **101**, 123905 (2008).
[17] N. N. Rosanov and V. E. Semenov, Opt. Spectrosc. **48**, 59 (1980).
[18] M. Tlidi, P. Mandel, and R. Lefever, Phys. Rev. Lett. **73**, 640 (1994).
[19] A. J. Scroggie *et al.*, Chaos, Solitons Fractals **4**, 1323 (1994).
[20] M. Tlidi and P. Mandel, Chaos, Solitons Fractals **4**, 1475 (1994).
[21] D. V. Skryabin and W. J. Firth, Opt. Lett. **24**, 1056 (1999).
[22] M. Tlidi, P. Mandel, and M. Haelterman, Phys. Rev. E **56**, 6524 (1997).
[23] C. Etrich, U. Peschel, and F. Lederer, Phys. Rev. E **56**, 4803 (1997).
[24] S. Longhi, Phys. Rev. A **59**, 4021 (1999).
[25] P. Lodahl, M. Bache, and M. Saffman, Opt. Lett. **25**, 654 (2000).
[26] A. G. Vladimirov, J. M. McSloy, D. V. Skryabin, and W. J. Firth, Phys. Rev. E **65**, 046606 (2002).
[27] M. Tlidi, P. Mandel, and R. Lefever, Phys. Rev. Lett. **81**, 979 (1998).
[28] N. N. Rosanov and G. V. Khodova, Opt. Spectrosc. **65**, 828 (1988).
[29] N. N. Rosanov and G. V. Khodova, J. Opt. Soc. Am. B **7**, 1057 (1990).
[30] S. Trillo, M. Haelterman, and A. Sheppard, Opt. Lett. **22**, 970 (1997).
[31] K. Staliunas and V. J. Sanchez-Morcillo, Phys. Lett. A **241**, 28 (1998).
[32] M. Le Berre, D. Leduc, E. Ressayre, and A. Tallet, J. Opt. B: Quantum Semiclassical Opt. **1**, 107 (1999).
[33] G. L. Oppo, A. J. Scroggie, and W. J. Firth, J. Opt. B: Quantum Semiclassical Opt. **1**, 133 (1999).
[34] M. Tlidi, M. Le Berre, E. Ressayre, A. Tallet, and L. Di Menza, Phys. Rev. A **61**, 043806 (2000).
[35] A. G. Vladimirov, G. V. Khodova, and N. N. Rosanov, Phys. Rev. E **63**, 056607 (2001).
[36] D. Gomila, P. Colet, G.-L. Oppo, and M. San Miguel, Phys. Rev. Lett. **87**, 194101 (2001).
[37] F. Mitschke, G. Steinmeyer, and A. Schwache, Physica D **96**, 251 (1996).
[38] S. Coen and M. Haelterman, Phys. Rev. Lett. **79**, 4139 (1997); S. Coen, M. Tlidi, Ph. Emplit, and M. Haelterman, *ibid.* **83**, 2328 (1999).
[39] M. Tlidi, A. Mussot, E. Louvergneaux, G. Kozyreff, A. G. Vladimirov, and M. Taki, Opt. Lett. **32**, 662 (2007); G. Kozyreff, M. Tlidi, A. Mussot, E. Louvergneaux, M. Taki, and A. G. Vladimirov, Phys. Rev. Lett. **102**, 043905 (2009).
[40] N. A. Kaliteevskii, N. N. Rosanov, and S. V. Fedorov, Opt. Spectrosc. **85**, 485 (1998).
[41] Y. Silberberg, Opt. Lett. **15**, 1282 (1990).
[42] H. Leblond, J. Opt. A, Pure Appl. Opt. **4**, 160 (2002).
[43] N. Akhmediev, J. M. Soto-Crespo, and P. Grelu, Chaos **17**, 037112 (2007).
[44] N. Akhmediev and J. M. Soto-Crespo, Phys. Rev. A **47**, 1358 (1993).
[45] P. M. Lushnikov and M. Saffman, Phys. Rev. E **62**, 5793 (2000).
[46] M. Tlidi, M. Haelterman, and P. Mandel, EPL **42**, 505 (1998).
[47] P. Tassin, G. Van der Sande, N. Veretenov, P. Kockaert, I. Veretennicoff, and M. Tlidi, Opt. Express **14**, 9338 (2006).
[48] K. Staliunas, Phys. Rev. Lett. **81**, 81 (1998).
[49] M. Tlidi and P. Mandel, Phys. Rev. Lett. **83**, 4995 (1999).
[50] Mustapha Tlidi, J. Opt. B: Quantum Semiclassical Opt. **2**, 438 (2000).
[51] M. Tlidi, D. Pieroux, and P. Mandel, Opt. Lett. **28**, 1698 (2003).
[52] S. Fedorov, N. Rosanov, A. Shatsev, N. Veretenov, and A. G. Vladimirov, IEEE J. Quantum Electron. **39**, 197 (2003).
[53] N. A. Veretenov, N. N. Rosanov, and S. V. Fedorov, Opt. Quantum Electron. **40**, 253 (2008).
[54] N. A. Veretenov, N. N. Rosanov, and S. V. Fedorov, Opt. Spectrosc. **104**, 563 (2008).
[55] J. M. Soto-Crespo, N. Akhmediev, N. Devine, and C. Mejia-Corts, Opt. Express **16**, 15388 (2008).
[56] D. Mihalache, D. Mazilu, F. Lederer, H. Leblond, and B. A. Malomed, Phys. Rev. E **78**, 056601 (2008).
[57] M. Brambilla, T. Maggipinto, G. Patera, and L. Columbo, Phys. Rev. Lett. **93**, 203901 (2004).
[58] L. Columbo, I. M. Perrini, T. Maggipinto, and M. Brambilla, New J. Phys. **8**, 312 (2006).
[59] C. L. Tang and L. K. Cheng, *Fundamentals of Optical Parametric Processes and Oscillators*, Laser Science and Technology Series Vol. 20 (Harwood Academic Publishers GmbH, Amsterdam, 1995).
[60] *Mid-infrared Coherent Sources and Applications*, edited by M. Ebrahim-Zadeh and I. T. Sorokina (Springer, New York, 2008).
[61] P. Tassin, L. Gelens, J. Danckaert, I. Veretennicoff, G. Van der Sande, P. Kockaert, and M. Tlidi, Chaos **17**, 037116 (2007).